Co-harvesting Solar Energy with Ambient Heat and On-Demand Release of Thermal Energy Below 0 °C Through Visible-Light-Controlled Photochemical Phase Transitions of Azopyrazoles

Zhichun Shangguan,[1] Wenjin Sun,[1] Zhao-Yang Zhang,[1] Dong Fang,[1] Si Wu,[2] Chao Deng,[3] Xianhui Huang,[1] Yixin He,[1] Ruzhu Wang,[2] Tingxian Li,[2] Tao Li*[1]

[1]School of Chemistry and Chemical Engineering, Frontiers Science Center for Transformative Molecules, Shanghai Key Laboratory of Electrical Insulation and Thermal Aging, Key Laboratory of Thin Film and Microfabrication (Ministry of Education), Shanghai Jiao Tong University, Shanghai 200240, China. *E-mail: litao1983@sjtu.edu.cn

[2]Research Center of Solar Power & Refrigeration, School of Mechanical Engineering, Shanghai Jiao Tong University, Shanghai 200240, China

[3]College of Chemistry & Materials Engineering, Wenzhou University, Wenzhou 325027, Zhejiang, China

Abstract

Photochemical crystal-to-liquid transition generally needs UV light as a stimulus and it is even more challenging to carry out below 0 °C. Here, we design a series of 4-alkylthioarylazopyrazoles as molecular solar thermal batteries, which show bidirectional visible-light-triggered photochemical *trans*-crystal ↔ *cis*-liquid transitions below ice point (-1 °C). Through co-harvesting visible-light energy and low-temperature ambient heat, high energy density (0.25 MJ kg^{-1}) is achieved. Further, the rechargeable solar thermal batteries devices are fabricated, which can be charged by blue light (400 nm) at -1 °C. Then, the charged devices can release energy on demand in the form of high-temperature heat. Under green light (532 nm) irradiation, the temperature difference between the charged devices and the ice-cold surrounding is up to 13.5 °C. This study paves the way for the design of advanced molecular solar thermal batteries that store both natural sunlight and ambient heat over a wide temperature range.

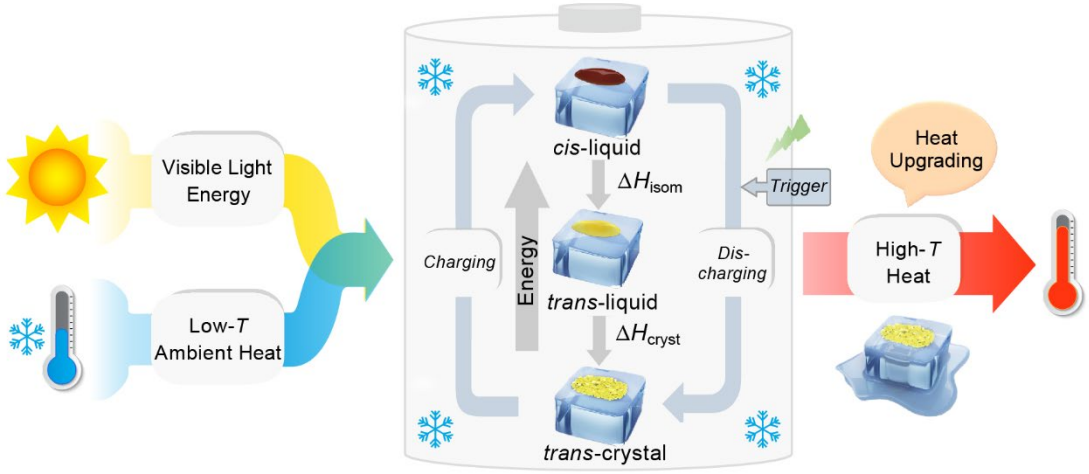

Introduction

The development of technologies for sustainable energy is essential to lead energy production away from fossil fuels. Solar energy comes from an almost inexhaustible source of sunlight and it is integral part of renewable energy. The intermittent and fluctuant characteristics of solar energy requires an energy storage system to achieve effective utilization.[1-3] Molecular solar thermal batteries have been recognized as a promising avenue to harvest and store solar energy in the form of chemical bonds.[4-6] In this approach, a photochromic molecule can be transformed into a high-energy metastable isomer through photoisomerization, which can subsequently be switched back to the original stable isomer upon exposure to external stimuli, accompanied by releasing stored energy in the form of heat. Several kinds of photochromic molecules have been studied for molecular solar thermal batteries, including azobenzenes[7-9], dihydroazulenes[10], fulvalene diruthenium[11-12], and norbornadienes[13-15]. Among these candidates, azobenzenes have gained increased attention due to their highly tunable absorption spectra, facile synthesis, and exceptional cycling stability.[16-20] However, the relatively low isomerization enthalpy (ΔH_{iso} ~ 41 kJ mol^{-1}) results in low energy density, and thus severely limits the application of pristine azobenzene in storing solar energy.[21] Some strategies have been employed to solve this problem, such as molecular engineering[22-23], template assembly[5, 24-26] and photochemical phase transitions[27-30]. Significantly, photochemical phase transitions enable co-harvesting photo energy and ambient heat through the transformation of azo molecules from *trans*-crystal to *cis*-liquid, and can release energy on demand as high-temperature heat by triggering the liquid-to-crystal transition. Moreover, the azo molecules possessing photochemical phase transition behavior can serve as "photon driven heat pumps" to upgrade the ambient heat.[27]

However, a general problem for the current reports of azobenzene photochemical phase transition systems is that photochemical crystal ↔ liquid transition (PCLT) requires UV light. While UV light comprises only a small fraction (4.5%) of the total solar spectrum[31], resulting in the weak solar energy utilization of azobenzene molecules. To date, only one study has reported the utilization of *ortho*-functionalized azobenzene derivatives to achieve visible- light-triggered PCLT, but the total energy densities are only 0.07 – 0.15 MJ kg^{-1}.[32] *Ortho*-substituted azobenzenes have increased energy of *trans*-isomers or decreased energy of *cis*-isomers, so that the ΔH_{iso} of them are only 6 – 25 kJ mol^{-1}, much lower than pristine azobenzene.[33-34] Therefore, the development of new visible-light-triggered PCLT molecular systems without reducing ΔH_{iso} is critical.

Another limitation for azo-based PCLT systems is their inability to directly store and release energy in cold environments, especially at or below 0 °C. The melting point (T_m) of most reported *cis*-isomers is in the range of 20 – 200 °C[35], which means the photoisomerization from *trans*-crystal to *cis*-liquid cannot occur at low ambient temperatures. Although some *cis*-isomers can release energy below 0 °C due to their supercooling behavior, the charging process is still at room temperature (27 °C).[27-28]

Here, we report new arylazopyrazoles as molecular solar thermal batteries, which show highly efficient PCLT triggered by visible light even below 0 °C, as illustrated in Figure 1. In addition, by storing both visible light energy and low-temperature ambient heat, a high gravimetric energy density of 0.25 MJ kg^{-1} is achieved. Further, the *cis*-isomer has a half-life of 22 days at 0 °C, indicating its stable thermal energy storage capacity. Finally, thin film devices are fabricated for solar thermal energy storage which can be readily charged and discharged at -1 °C with 400 nm blue light and 532 nm green light, respectively, and the surface temperature of charged devices can reach

up to 12.5 °C during green light irradiation. Direct charging and discharging energy at such low temperatures has significant implications for deicing and home heating under ice-cold conditions, thus reducing the energy consumption of conventional heating.

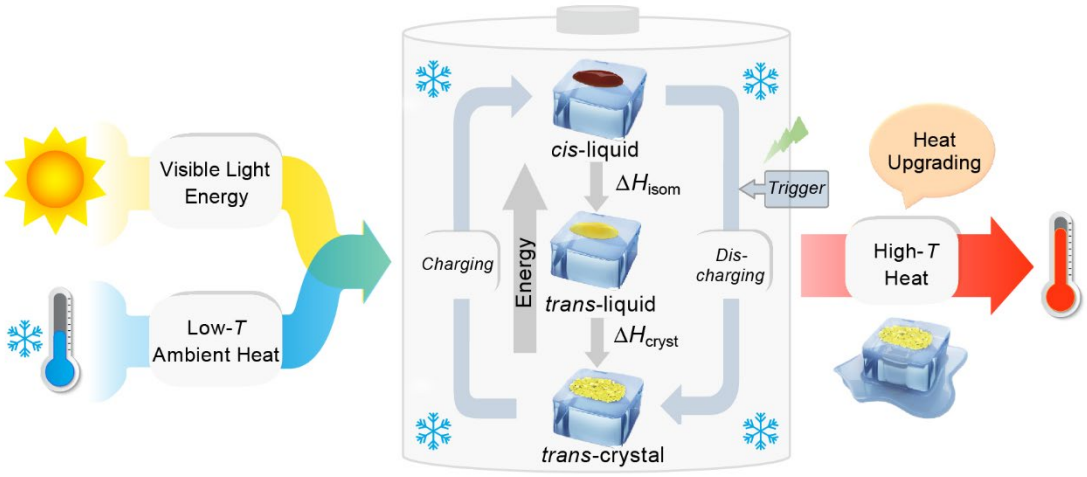

Figure 1. Schematic representation of reversible photochemical crystal ↔ liquid transitions below 0 °C of an azo-based molecular solar thermal battery that store energy from both visible light and low-temperature ambient heat, and then releases on demand in the form of high-temperature heat.

Results and Discussion

The introduction of a 4-thiomethyl group and changing the bridging positions between the azo group and pyrazole ring was expected to achieve bidirectional visible light switching through extending the π-conjugation. According, three 4-methylthioarylazopyrazoles (S3, S4, and S5) were designed and synthesized by a diazo coupling reaction or Mills reaction (Scheme S1), as shown in Figure 2a. Their photoisomerization behaviors were studied by UV-Vis absorption spectra in an acetonitrile solution. As shown in Figure 2, all *trans*-isomers exhibited single and intense absorption bands in 350 – 400 nm region (ε_{max} = 25 – 32×10^3 M^{-1} cm^{-1}) due to π-π* transition. Compared with the reported 4-methoxyarylazopyrazole (O4, 342 nm)[36], the π-π* λ_{max} of S3 and S4 were red-shifted to about 360 nm, and further to 385 nm for S5 (Table S1). The *trans*/*cis* relative absorption of S3, S4 and S5 at 400 nm was strong (Table S1), and hence it was possible to realize *trans*-to-*cis* isomerization by visible light. The photostationary states (PSSs) at different wavelengths (from 365 to 532 nm) were studied (Figure S1), and the isomeric compositions were presented in Table S2. As a result, 400 nm blue light induced near-quantitative yield (> 95%) of *trans*-to-*cis* isomerization for S5, while only ~85% for S3 and S4. The higher *trans*-to-*cis* photoconversion of S5 was attributed to its π-π* λ_{max} closer to 400 nm and stronger *trans/cis* relative absorption at λ = 400 nm. Exciting the tail of n-π* bands of three *cis*-isomers by green light (532 nm) resulted in *cis*-to-*trans* isomerization. The high overlap between the n-π* band of *cis*-S4 and the long-wavelength absorption band of *trans*-S4 led to a relatively low *cis*-to-*trans* conversion (85%). In contrast to *cis*-S4, *cis*-S3 and *cis*-S5 exhibited n-π* transitions red-shifted of 25 nm and 36 nm (Table S1), respectively, which led to partial separation of n-π* bands of the *cis* and *trans* isomers, thereby inducing high (92% S3) to near-quantitative (> 95% S5) isomerization.

On this basis, the geometries of **O4**, **S3**, **S4**, and **S5** as well as their electronic transition characteristics were calculated to evaluate the relationship between molecular structures and photophysical properties (see Section 3 in SI). All *trans*-isomers exhibited a planar structure with a

C-N-N-C dihedral angle of 180.0° (Figures 2e and S5), which resulted in symmetry-forbidden of n-π* transitions ($S_0 \rightarrow S_1$) with negligible oscillator strength ($f = 0.00$, Table S4). Compared with *trans*-**O4**, 4-methylthioarylazopyrazoles series showed more effective extension of the π-conjugated system due to the increase of p-π conjugation by introducing the 4-SMe group[37-38], as indicated by their frontier molecular orbitals (Figures S7-S10). Consequently, the energy gap between HOMO (π orbital) and LUMO (π* orbital) were smaller for 4-methylthioarylazopyrazoles series) (3.714, 3.776, and 3.542 eV for S3, S4, and S5, respectively, as depicted in Figure 2f, leading to the bathochromic shift of their π-π* transition ($S_0 \rightarrow S_2$). The more red-shift of S5 was caused by a "complete" conjugation pathway between 5-pyrazole and the azo group that further expands the π-conjugation of the system.[39-40] *Cis*-S4 showed nearly T-shaped conformation with a C-C-N-N dihedral angle of 82.8° (Figures 2e and S5), resulting in a weak n-π* transition with *f* of only 0.0048. While *cis*-S3 and *cis*-S5 were found to disfavor the T-shaped conformation owing to the presence of the ortho nitrogen atom (Figures 2e and S5). Therefore, their n-π* absorbance bands were remarkably enhanced (f = 0.1068 and 0.1096 for *cis*-S3 and *cis*-S5, respectively, Table S4), and nearly quantitative conversions from *cis* to *trans* isomers were achieved.

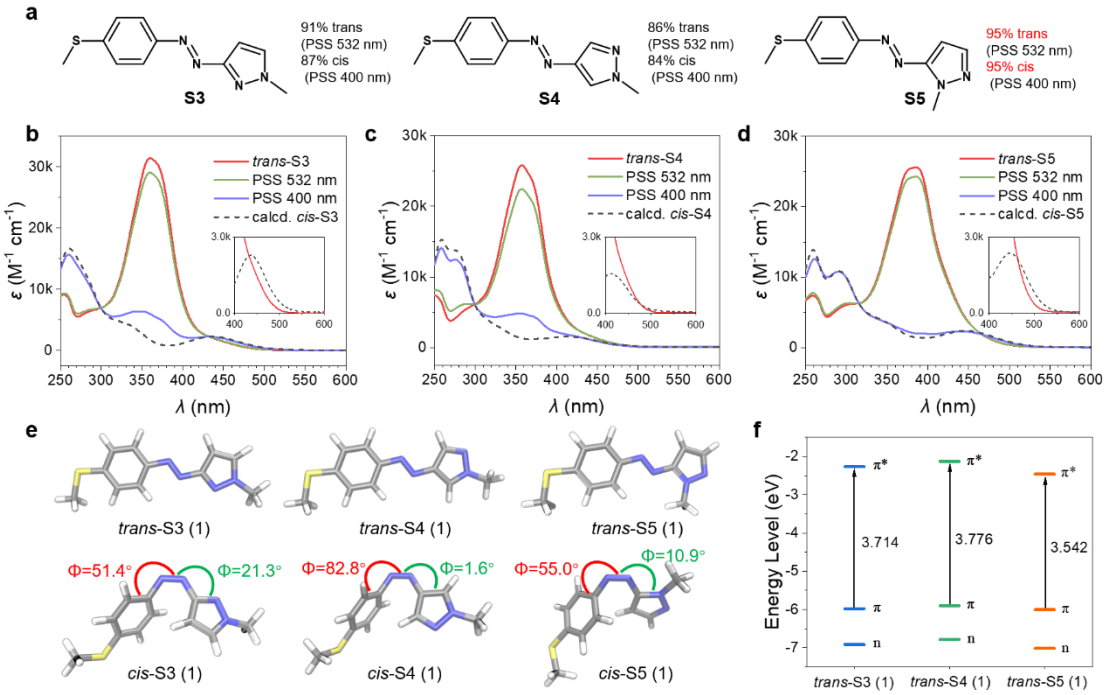

Figure 2. (a) Structures of 4-methoxyarylazopyrazole and their PSSs at 400 nm and 532 nm. Photoisomerization of (b) **S3**, (c) **S4**, and (d) **S5** measured in acetonitrile, insets show the zoomed-in spectra of n-π* regions. (e) The geometric optimized structure of 4-methoxyarylazopyrazole (calculations were performed at PBE0-D3(BJ)/6-31G** level of theory in gas). (f) Calculated energy diagram of the π, n, and π* orbitals.

Thus, all these data indicated that **S5** can be used as a bi-directional visible-light-driven photoswitch, which provided near-quantitative *trans*-to-*cis* and *cis*-to-*trans* photoconversions in acetonitrile solution. However, pristine **S5** was not able to store both visible-light energy and phase changes latent heat at low temperature since its PCLT was inhibited even at room temperature. To achieve PCLT below 0 °C, two principles should be considered: (1) the *trans*-isomer has a T_m and crystallization point (T_{cry})much higher than 0 °C, thus forming crystals. (2) The T_m of *cis*-isomer is below 0 °C, thus forming amorphous liquids. We varied the length of linear alkyl chains with or

without a vinylic end group on alkylthio group, denoted as **An-S5** and **Bn-S5** (Figure 3a and Scheme S2). As shown in Figures3b, 3c, S11 and S12, the *trans*-isomers with longer and intermediate alkyl chain lengths (n = 6 – 12 for An-S5, and n= 7, 9, 11 for Bn-S5) showed T_m (40 – 60 °C) and T_{cry} above 0 °C (10 – 45 °C, Table S5 and S6). The *cis*-isomers with intermediate alkyl chain lengths had the lowest T_m (5 °C for A6-S5 and -1 °C for B7-S5), as shown in Figures 3b, 3c, S13 and S14. Hence, B7-S5 could undergo visible-light-triggered PCLT in cold environments thanks to its low *cis*-isomer T_m (below 0 °C) and high *trans*-isomer T_{cry} (34 °C). This property allowed it to store energy from both visible light and low-temperature ambient heat.

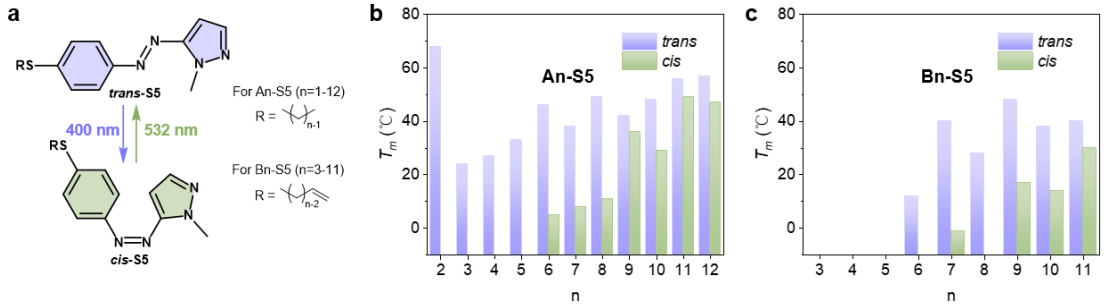

Figure 3. (a) The structures of **An-S5** and **Bn-S5**. The T_m of *trans* and *cis* isomer of (b) **An-S5** and (c) **Bn-S5**.

The reversible PCLTs of **B7-S5** at -1 °C were discussed as follows. As shown in Figure 4a and Video S1, after 400 nm light irradiation, the *trans*-**B7-S5** in the orange crystal state lost birefringence and was melted into red liquids which then switched back to a crystal state by 532 nm light irradiation. UV-Vis spectra were used to record the photoisomerization yields during irradiation of a neat sample of **B7-S5**. During the photo-melting process (Figure 4b), the *trans*-to-*cis* isomerization of **B7-S5** in a neat state proceed easily and produced a high yield of photoisomerization (92.5%) at 40 min, slightly lower than that in dilute solutions (> 95%). For the photo-crystallization process (Figure 4c), the *trans*-isomer content of the sample increased exponentially, and a near-quantitative (95.4%) *cis*-to-*trans* isomerization was achieved within 2 min of irradiation. X-ray diffraction (XRD) analyses were carried out to further verify the reversible PCLT behaviors of **B7-S5** (Figure 4d). The sharp peaks at 2θ of 5-35° before irradiation corresponded to the regular stack of azo molecules in crystals. After exposure to 400 nm light, the peaks disappeared, indicating that *cis*-**B7-S5** had an amorphous structure. Subsequently, XRD patterns were recovered, when the sample was irradiated with 532 nm light. X-ray crystal structure of *trans*-**B7-S5** reveals an antiparallel packing, and several weak contacts such as alkyl-alkyl, alkyl-phenyl, and alkyl-pyrazolyl dominating the intermolecular interactions (Figure 4e). Presumably, the absence of strong intermolecular interactions in *trans*-**B7-S5** was beneficial for PCLTs.[41-42] Such efficient bidirectional visible-light-triggered PCLTs at -1 °C underlined the advantage of **B7-S5** in utilizing solar and ambient energy at low temperatures.

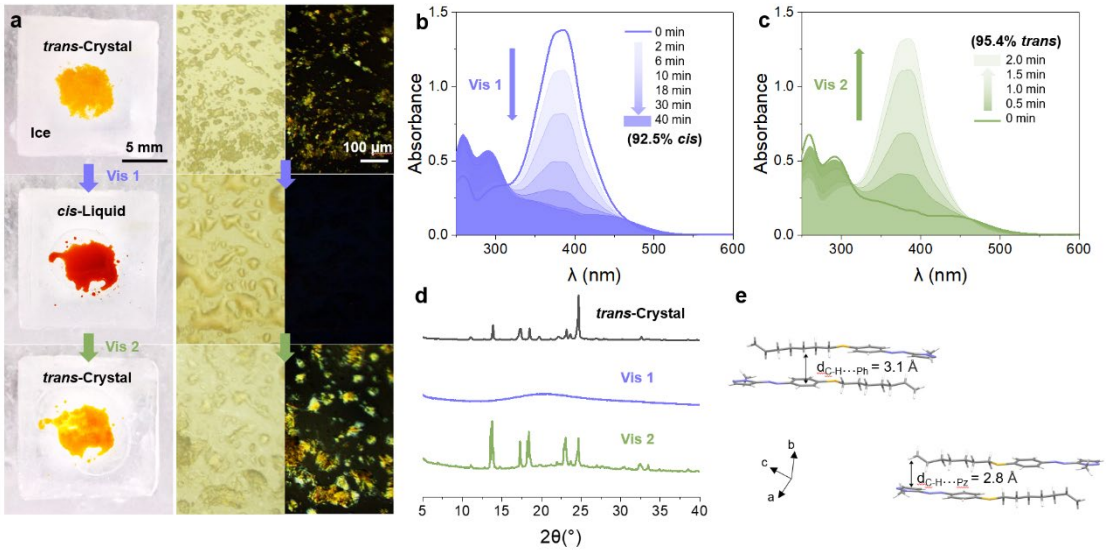

Figure 4. (a) Photographs, optical microscopy images, and POM image of **B7-S5** on ice surface. From top to bottom panels are *trans*-crystals before irradiation, *cis*-liquids after 400 nm light irradiation, and regenerated *trans*-crystals after subsequent irradiation by 532 nm light. UV−vis absorption spectra change during (b) 400 nm and (c) 532 nm light irradiation of neat **B7-S5** at -1 °C. (d) XRD patterns change of **B7-S5** on glass slides during PCLTs at -1 °C. (e) Crystal packing structure of *trans*-**B7-S5**.

The *cis*-isomer of azobenzene can be thermally relaxed into *trans*-isomer in the dark spontaneously, which determines the energy storage time of molecular solar thermal batteries. The change of absorbance value at π-π* λ_{max} (385 nm) as a function of time was measured in acetonitrile solution between 25 and 40 °C (Figure 5a). The thermal isomerization rate constants, $k_{cis\rightarrow trans}$, were calculated based on the first-order reaction kinetics at 25 °C, 30 °C, 35 °C, and 40 °C, respectively. Based on the Eyring equation, the thermodynamic parameters were obtained with $\Delta H^{\ddagger}$ = 115 kJ mol^{-1}, $\Delta S^{\ddagger} = -13$ J K^{-1} mol^{-1}. Thus, *cis*-**B7-S5** was found to have a half-life $t_{1/2}$ of 22 days at 0 °C, indicating its stable thermal energy storage capacity at low temperatures. Additionally, the **B7-S5** demonstrated excellent photon-harvesting ability with the quantum yield $\Phi_{trans\rightarrow cis}$ of 0.39 ± 0.01 for photoisomerization in acetonitrile solution (Figure S15), similar to other reported azopyrazoles compounds[27, 40, 43].

To evaluate the energy storage capacity of the *cis*-liquid **B7-S5**, the isomerization enthalpy ΔH_{iso} of thermally induced *cis*-liquid to *trans*-liquid reversion reaction, and crystallization enthalpy ΔH_{cry} of *trans*-liquid to *trans*-solid transition were measured by differential scanning calorimetry (DSC). As shown in Figure 5b, the *cis*-**B7-S5** liquid revealed a broad exothermic peak over 60-120 °C during the thermally activated *cis*-to-*trans* isomerization, and the integrated area under the peak represented ΔH_{iso} of 0.14 MJ kg^{-1} (44 kJ mol^{-1}). This result was consistent with our calculation (49 kJ mol^{-1}, Table S7) based on density functional theory (DFT), and it was slightly higher than that of pristine azobenzene (41 kJ mol^{-1}). Furthermore, the DSC cooling curve displayed a sharp exothermic peak at around 33 °C with ΔH_{cry} of 0.11 MJ kg^{-1} (35 kJ mol^{-1}), which was due to the *trans*-liquid to *trans*-solid transition. Therefore, the total thermal energy storage density of *cis*-B7-S5 was 0.25 MJ kg^{-1} (79 kJ mol^{-1}). According to $\Phi_{trans\rightarrow cis}$ and ΔH_{iso}, the solar efficiency η was estimated to be 1.3% (see Section 5 in SI), which was one of the highest values reported for azo-based molecular solar thermal batteries (0.2-1.3%)[27, 32].

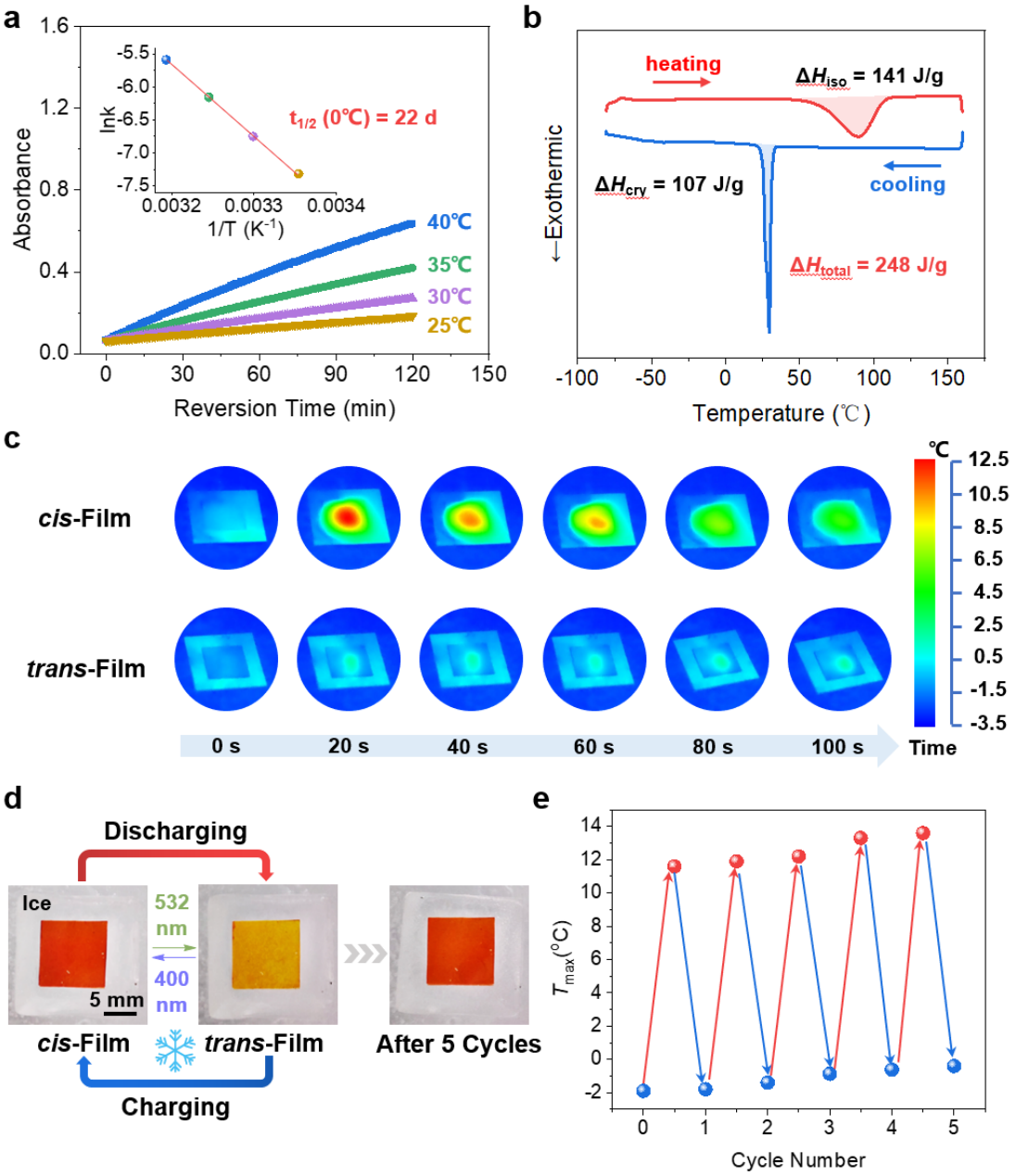

Figure 5. (a) Thermal *cis–trans* recovery of *cis*-**B7-S5** in acetonitrile with time at different temperatures followed by the absorbance increase at λ_{max} = 385 nm, inset shows the linear fit between ln*k* and 1/*T* according to the Arrhenius equation. (b) First heating (red) and subsequent cooling DSC curves (blue) of *cis*-**B7-S5**. (c) Time-evolved infrared images of the *cis*-**B7-S5** and *trans*-**B7-S5** under 532 nm light irradiation at -1 °C. (d) Photographs of the *cis* and *trans* film, the left show the photograph of *cis*-film after five cycles. (e) The maximum heat release during five charging/discharging cycles under 532 nm light irradiation.

Owing to the fast transition of *cis*-liquid to *trans*-crystal triggered by green light, the energy of ΔH_{iso} and ΔH_{cry} were released on demand and rapidly. In order to distinctly demonstrate the heat release process at low temperature, a high-resolution infrared thermal imaging camera was used to track the temperature changes of a 1 cm^2 size film containing 5 mg of *cis*-**B7-S5** (fabricated using the method we previously reported[27]) exposed to 532 nm green light when the ambient temperature was -1 °C (Figure 5c, Video S2). Once irradiated, the film immediately released heat and the

maximum surface temperature that generally appeared at the central region of film reached 12.5 ºC at 20 s, about 13.5 ºC higher than the surroundings. Such high-*T* heat release also means that **B7-S5** can act as a photon-driven molecular heat pump, upgrading thermal energy from low to high temperature. Moreover, at low temperature (-1 ºC), this solar thermal battery film could be directly recharged and discharged by alternating 400 nm and 532 nm light irradiations. No destruction of film morphology or reduction in heat release was observed in five charge and discharge cycles (Figures 5d and 5e). These solar thermal battery devices show unprecedented performances, including visible-light storage, ice-cold working, energetic, and recyclable, which are an ideal candidate for future energy management systems.

Conclusion

In conclusion, we have successfully designed a series of bidirectional visible-light switching azo molecules and applied them for storing and releasing solar energy in cold environments. The 4-thiomethyl group effectively extends the π-conjugated system through p-π conjugation, which significantly red-shifts the π-π* absorption bands of azo molecules. The photoswitch properties can be further tuned by changing the connection position (C3, C4, or C5 positions) of the pyrazole ring and the azo group. **S5** shows near-quantitative bidirectional isomerization under visible light due to the combination of electronic effects (the highest π-conjugation degree) and the geometrical conformation of *cis* isomers (disfavor the T-shaped conformation). Moreover, the reversible visible-light-triggered PCLTs have been achieved below 0 ºC by optimizing the length of linear alkyl chains with or without a vinylic end group on alkylthio groups. Accordingly, the azo photoswitches could not only store the visible-light energy and low-temperature ambient heat simultaneously but also display controlled and on-demand heat release. Under green light irradiation, the molecules released high density heat (0.25 MJ kg^{-1}), and the film devices produced a temperature lift of up to 13.5 ºC from the ambient temperature. Thus, this work may open an avenue for the design of advanced molecular solar thermal systems that store natural sunlight and ambient heat over a wide temperature range.

Supporting Information

Additional Figures, Synthesis details, DFT calculation details, and characterization data (PDF)
Video S1, photochemical phase transitions of **B7-S5** at -1 °C (MP4)
Video S2, heat release of *cis*-film sample on ice surface under 532 nm light irradiation (MP4)
Video S3, heat release of *trans*-film sample on ice surface under 532 nm light irradiation (MP4)

Acknowledgements

This work was supported by the National Key Research and Development Program of China (2017YFA0207500), National Natural Science Foundation of China (22022507, 51973111), Beijing National Laboratory for Molecular Sciences (BNLMS202004) and China Postdoctoral Science Foundation (2020M681279).

References

(1) J. Gong, C. Li, M. R. Wasielewski, *Chem. Soc. Rev.* **2019**, *48*, 1862-1864.

(2) T. R. Cook, D. K. Dogutan, S. Y. Reece, Y. Surendranath, T. S. Teets, D. G. Nocera, *Chem. Rev.* **2010**, *110*, 6474-6502.

(3) S. Wu, T. Li, Z. Tong, J. Chao, T. Zhai, J. Xu, T. Yan, M. Wu, Z. Xu, H. Bao, T. Deng, R. Wang,

Adv. Mater. **2019**, *31*, 1905099.

(4) T. J. Kucharski, Y. Tian, S. Akbulatov, R. Boulatov, *Energy Environ. Sci.* **2011**, *4*, 4449-4472.

(5) T. J. Kucharski, N. Ferralis, A. M. Kolpak, J. O. Zheng, D. G. Nocera, J. C. Grossman, *Nat. Chem.* **2014**, *6*, 441-447.

(6) C.-L. Sun, C. Wang, R. Boulatov, *ChemPhotoChem* **2019**, *3*, 268-283.

(7) L. Dong, Y. Feng, L. Wang, W. Feng, *Chem. Soc. Rev.* **2018**, *47*, 7339-7368.

(8) S. Wu, H.-J. Butt, *Macromol. Rapid Commun.* **2020**, *41*, 1900413.

(9) K. Masutani, M.-a. Morikawa, N. Kimizuka, *Chem. Commun.* **2014**, *50*, 15803-15806.

(10) S. L. Broman, M. Å. Petersen, C. G. Tortzen, A. Kadziola, K. Kilså, M. B. Nielsen, *J. Am. Chem. Soc.* **2010**, *132*, 9165-9174.

(11) K. Moth-Poulsen, D. Ćoso, K. Börjesson, N. Vinokurov, S. K. Meier, A. Majumdar, K. P. C. Vollhardt, R. A. Segalman, *Energy Environ. Sci.* **2012**, *5*, 8534-8537.

(12) Y. Kanai, V. Srinivasan, S. K. Meier, K. P. C. Vollhardt, J. C. Grossman, *Angew. Chem. Int. Ed.* **2010**, *49*, 8926-8929.

(13) J. Orrego-Hernández, A. Dreos, K. Moth-Poulsen, *Acc. Chem. Res.* **2020**, *53*, 1478-1487.

(14) Z. Wang, A. Roffey, R. Losantos, A. Lennartson, M. Jevric, A. U. Petersen, M. Quant, A. Dreos, X. Wen, D. Sampedro, K. Börjesson, K. Moth-Poulsen, *Energy Environ. Sci.* **2019**, *12*, 187-193.

(15) A. Kunz, H. A. Wegner, *ChemSystemsChem* **2021**, *3*, e2000035.

(16) S. Crespi, N. A. Simeth, B. König, *Nat. Rev. Chem.* **2019**, *3*, 133-146.

(17) H. M. D. Bandara, S. C. Burdette, *Chem. Soc. Rev.* **2012**, *41*, 1809-1825.

(18) Z. Shangguan, C. Yu, C. Li, X. Huang, Y. Mai, T. Li, *J. Mater. Chem. C* **2020**, *8*, 10837-10843.

(19) D. Fang, Z.-Y. Zhang, Z. Shangguan, Y. He, C. Yu, T. Li, *J. Am. Chem. Soc.* **2021**, *143*, 14502-14510.

(20) C.-Y. Shi, Q. Zhang, H. Tian, D.-H. Qu, *SmartMat* **2020**, *1*, e1012.

(21) R. J. Corruccini, E. C. Gilbert, *J. Am. Chem. Soc.* **1939**, *61*, 2925-2927.

(22) E. Durgun, J. C. Grossman, *J. Phys. Chem. Lett.* **2013**, *4*, 854-860.

(23) W. Moormann, T. Tellkamp, E. Stadler, F. Röhricht, C. Näther, R. Puttreddy, K. Rissanen, G. Gescheidt, R. Herges, *Angew. Chem. Int. Ed.* **2020**, *59*, 15081-15086.

(24) H. Wang, Y. Feng, H. Yu, L. Dong, F. Zhai, J. Tang, J. Ge, W. Feng, *Nano Energy* **2021**, *89*, 106401.

(25) W. Yang, Y. Feng, Q. Si, Q. Yan, P. Long, L. Dong, L. Fu, W. Feng, *J. Mater. Chem. A* **2019**, *7*, 97-106.

(26) A. M. Kolpak, J. C. Grossman, *Nano Lett.* **2011**, *11*, 3156-3162.

(27) Z.-Y. Zhang, Y. He, Z. Wang, J. Xu, M. Xie, P. Tao, D. Ji, K. Moth-Poulsen, T. Li, *J. Am. Chem. Soc.* **2020**, *142*, 12256-12264.

(28) M. A. Gerkman, R. S. L. Gibson, J. Calbo, Y. Shi, M. J. Fuchter, G. G. D. Han, *J. Am. Chem. Soc.* **2020**, *142*, 8688-8695.

(29) H. Liu, J. Tang, L. Dong, H. Wang, T. Xu, W. Gao, F. Zhai, Y. Feng, W. Feng, *Adv. Funct. Mater.* **2021**, *31*, 2008496.

(30) K. Ishiba, M.-a. Morikawa, C. Chikara, T. Yamada, K. Iwase, M. Kawakita, N. Kimizuka, *Angew. Chem. Int. Ed.* **2015**, *54*, 1532-1536.

(31) A. K. Saydjari, P. Weis, S. Wu, *Adv. Energy Mater.* **2017**, *7*, 1601622.

(32) Y. Shi, M. A. Gerkman, Q. Qiu, S. Zhang, G. G. D. Han, *J. Mater. Chem. A* **2021**, *9*, 9798-9808.

(33) A. A. Beharry, O. Sadovski, G. A. Woolley, *J. Am. Chem. Soc.* **2011**, *133*, 19684-19687.

(34) D. Bléger, J. Schwarz, A. M. Brouwer, S. Hecht, *J. Am. Chem. Soc.* **2012**, *134*, 20597-20600.

(35) W.-C. Xu, S. Sun, S. Wu, *Angew. Chem. Int. Ed.* **2019**, *58*, 9712-9740.

(36) Z.-Y. Zhang, Y. He, Y. Zhou, C. Yu, L. Han, T. Li, *Chem. Eur. J.* **2019**, *25*, 13402-13410.

(37) S. Bhunia, A. Dolai, S. Samanta, *Chem. Commun.* **2020**, *56*, 10247-10250.

(38) X. Xu, B. Wu, P. Zhang, Y. Xing, K. Shi, W. Fang, H. Yu, G. Wang, *ACS Appl. Mater. Interfaces* **2021**, *13*, 22655-22663.

(39) Y. He, Z. Shangguan, Z.-Y. Zhang, M. Xie, C. Yu, T. Li, *Angew. Chem. Int. Ed.* **2021**, *60*, 16539-16546.

(40) J. Calbo, C. E. Weston, A. J. P. White, H. S. Rzepa, J. Contreras-García, M. J. Fuchter, *J. Am. Chem. Soc.* **2017**, *139*, 1261-1274.

(41) P. Kumar, A. Srivastava, C. Sah, S. Devi, S. Venkataramani, *Chem. Eur. J.* **2019**, *25*, 11924-11932.

(42) L. Kortekaas, J. Simke, D. W. Kurka, B. J. Ravoo, *ACS Appl. Mater. Interfaces* **2020**, *12*, 32054-32060.

(43) C. E. Weston, R. D. Richardson, P. R. Haycock, A. J. P. White, M. J. Fuchter, *J. Am. Chem. Soc.* **2014**, *136*, 11878-11881.